

# Electronic band structure of low-temperature $\text{YB}_{12}$ , $\text{YB}_6$ superconductors and layered $\text{YB}_2$ , $\text{MgB}_2$ diborides

I.R. Shein\*, S.V. Okatov, N.I. Medvedeva and A.L. Ivanovskii

Institute of Solid State Chemistry, Ural Branch of the Russian Academy of Sciences, 620219, Ekaterinburg, Russia

Electronic band structure of boron-rich low-temperature superconductors  $\text{UB}_{12}$ -like dodecaboride  $\text{YB}_{12}$  and  $\text{CaB}_6$ -like hexaboride  $\text{YB}_6$  are investigated using the first-principle FLMTO calculations and compared with one for layered  $\text{YB}_2$  and the new "medium- $T_c$ " superconductor  $\text{MgB}_2$  diborides.

PACS: 71.15.La, 74.25.Jb

Keywords: electronic band structure, superconductors, hexaboride, dodecaboride.

## 1. Introduction

The discovery of the superconductivity in  $\text{MgB}_2$  ( $T_C \approx 40$  K) [1] and creation of promising materials based thereon (in the form of single crystals, ceramics, thin films, tapes and wires, see reviews [2,3] have attracted a great deal of interest in superconducting properties of other boron-containing phases.

Comparison between different classes of binary (semi- $(\text{M}_2\text{B})$ , mono- $(\text{MB})$ , di- $(\text{MB}_2)$ , tetra- $(\text{MB}_4)$ ) and some highest borides (hexa- $(\text{MB}_6)$ , dodeca- $(\text{MB}_{12})$  and  $\text{MB}_{66}$ -like borides), ternary and quaternary borides (review [3]) shows that the majority of known superconductors (SC) are found among low-boron-containing compounds ( $\text{B}/\text{M} \leq 2 - 2.5$ ), in which B atoms are in the form of isolated groups (atoms) or planar sublattices (boron sheets). The superconducting state is far less typical of highest borides ( $\text{B}/\text{M} \geq 6$ ) having a structure made up of stable polyhedra of boron atoms (octahedra  $\text{B}_6$  ( $\text{MB}_6$ ), icosahedra  $\text{B}_{12}$  ( $\text{MB}_{12}$ ) or their combination ( $\text{MB}_{66}$ )). Among a large number of these boron-rich phases, the low-temperature superconductivity was observed only for eight compounds:  $\text{MB}_6$  ( $\text{M} = \text{Y}$ ,  $\text{La}$ ,  $\text{Th}$ ,  $\text{Nd}$ ) and  $\text{MB}_{12}$  ( $\text{M} = \text{Sc}$ ,  $\text{Y}$ ,  $\text{Zr}$ ,  $\text{Lu}$ ) [3]. It is significant that (i) lower borides of these met-

als, in particular Sc and Y diborides, are not SC, and (ii) the stable polymorphy of the elemental boron ( $\alpha$ - $\text{B}_{12}$ ,  $\beta$ - $\text{B}_{105}$ ), which under equilibrium conditions contain the boron polyhedra (icosahedra or "gigantic" icosahedra  $\text{B}_{84}$ ) as structural elements, are semiconductors [4-8]. Only recently it was found that polycrystalline boron (rhombohedral  $\beta$ - $\text{B}_{105}$ ) transforms from a semiconductor to a superconductor ( $T_c \approx 11.2$  K) at about 250 GPa [9]. In this work we calculate the electronic band structures of low-temperature SCs - boron-rich phases  $\text{YB}_{12}$  and  $\text{YB}_6$  - and compare them with two representatives of layered  $\text{AlB}_2$ -type diborides, namely the non-superconducting  $\text{YB}_2$  and new "medium- $T_c$ " SC  $\text{MgB}_2$ . The results obtained are analyzed in terms of (i) electronic bands, (ii) density of states (DOS) and (iii) site-projected l-decomposed DOS near the Fermi energy ( $E_F$ ) of these borides. The Fermi surfaces for  $\text{YB}_2$  and  $\text{MgB}_2$  are also presented.

## 2. Structures and computational

The basic structural elements of the cubic dodecaboride  $\text{YB}_{12}$  are stable polyatomic boron clusters with icosahedral symmetry ( $\text{B}_{12}$ ) similar to that in elemental boron. The structure of the  $\text{UB}_{12}$  type (space group is  $\text{O}_h^5$ - $\text{Fm}\bar{3}\text{m}$ ) is formally described in terms of simple rock-salt lattice, where Y occupies Na sites and  $\text{B}_{12}$  icosahedra

\*E-mail: shein@ihim.uran.ru

dra are located in Cl sites, the unit cell contains 52 atoms ( $Z = 4$ ). The atomic positions are 4M (a) 0,0,0; 48B (i)  $\frac{1}{2}$ , x, x ( $x = 0.17011$  for our self-consistent calculation).

The role of Y and  $B_{12}$  in forming the  $YB_{12}$  band structure can be elucidated by removing Y atoms from the lattice entirely and calculating this hypothetical "dodecaboride" with an empty Y-sublattice ( $EB_{12}$  - E - structure vacancy) and the icosahedral phase ( $BB_{12}$ ), which is a result of the  $Y \rightarrow B$  substitution.

Yttrium hexaboride has a  $CaB_6$ -type structure (space group is  $O^1_h$ -Pm3m). It can be formally described in terms of a simple CsCl lattice, where metal atoms occupy Cs sites, while  $B_6$  octahedra are in Cl sites. The unit cell contains 7 atoms ( $Z = 1$ ). The atomic positions are M(a) 0,0,0; 6B(f)  $\frac{1}{2}$ ,  $\frac{1}{2}$ , x ( $x = 0.19538$  for our self-consistent calculation). There are two different B-B distances for intra- and inter-octahedral B-B bonds.

The crystal structure of layered  $AlB_2$ -like Mg and Y diborides (space group is  $D^1_{6h}$ -P6/mmm) is of an entirely different. It contains graphite-type boron sheets separated by hexagonal close-packed metal layers. Metal atoms are located at the center of hexagons formed by boron atoms. The unit cell contains 3 atoms ( $Z = 1$ ). The atomic positions are M (a): 0,0,0; 2B (d):  $\frac{1}{3}$ ,  $\frac{2}{3}$ ,  $\frac{1}{2}$  and  $\frac{2}{3}$ ,  $\frac{1}{3}$ ,  $\frac{1}{2}$ .  $AlB_2$ -type diborides exhibit a strong anisotropy of B-B bond lengths: the inter-plane distances are considerably higher than in-plane B-B distances. Table 1 lists the lattice parameters of the borides under study both taken from experiments [10] and obtained in our structural relaxation calculations.

The electronic band structures of the above-mentioned yttrium and magnesium borides were calculated using codes [11]. This program employs a scalar relativistic self-consistent full-potential linear muffin-tin method (FLMTO) within the local density approximation (LDA) [12] with allowance for correlation and exchange effects [13] by using the generalized gradient approximation (GGA) [14]. The tetrahedron method was used to calculate the density of states.

### 3. Results and discussion

#### 3.1. $YB_{12}$

Fig. 1 displays the energy bands of  $YB_{12}$  as compared with the hypothetical "dodecaboride"  $EB_{12}$  with a vacant Y sublattice. For  $EB_{12}$ , the total width of the valence band (VB) is 10.32 eV (without quasi-core B2s-type flat bands located at  $\sim 14$  eV below the Fermi level). It includes two groups of occupied hybrid B2s,2p-like bands (A and B) within the intervals  $-10.99 \div -8.83$  and  $-8.44 \div 0$  eV, separated by a gap ( $\sim 0.4$  eV). The lower bands contain predominately B2s-, and the upper bands - B2p-type contributions. The latter can be separated into three groups depending on the intra-atomic bonds in the crystal. There are two types of bonding B2s,2p states in the spectrum of  $EB_{12}$ . The states of the first type (covalent intra-icosahedral B-B interactions, namely three-center bonds on the triangular faces of icosahedra) are responsible for the stabilization of individual  $B_{12}$  polyhedra and depend little on the their packing ( $B_{12}$  sublattice structures) and the interaction of  $B_{12}$  between each other (as well as with second sublattice atoms). They correspond to high k-dispersion bonding bands located below  $E_F$  and are similar for  $BB_{12}$  and  $YB_{12}$ , see Fig. 1,2.

The states of the second group involve inter-icosahedral interactions. The nonbonding 2s,2p states of boron atoms surrounding the vacant sites in  $B_{12}$  belong to third group. The narrow B' and B" peaks in DOS correspond to it. These states form, in particular, a set of very flat partially occupied bands near the Fermi level (peak B") with large effective masses. Consequently,  $EB_{12}$  is a metal similar to  $\alpha$ - $B_{50}$  [7]. As distinct from the stable insulating state of  $\alpha$ - $B_{12}$  [5-8], where all mentioned above bands are fully occupied, the "deficiency" of electrons determining the metal-like properties of the hypothetical  $EB_{12}$  is brought about by structural peculiarities of the modeling  $B_{12}$  crystal. There are "empty spheres" in its bulk on the place of removed Y atoms. This intrinsic hole region accumulates some electrons (0.95 e according to our estimates) leading to partial devastation of the upper boron bands. DOS at the Fermi level ( $N(E_F) = 6.177$  eV/cell) con-

sist of mainly B2p component ( $\sim 96$  percentage). The spectrum of  $\text{EB}_{12}$  contains a wide forbidden band of 1.36 eV (FG, direct transition in X point) comparable with the FG in  $\alpha$ - $\text{B}_{12}$  (indirect  $\Gamma \rightarrow \text{Z}$  gap of  $\sim 1.43 - 1.70$  eV [5-8]).

The main differences in band structures of  $\text{YB}_{12}$  and  $\text{EB}_{12}$  are determined by valence yttrium s,p,d-states hybridized with above mentioned inter-icosahedra and nonbonding B2p states, peak C Fig. 2. For  $\text{YB}_{12}$ , the total width of the valence band is 12.98 eV, including two groups of fully occupied hybrid B2s,2p bands of 2.82 and 8.89 eV widths separated by a pseudogap. These bands shows the significant dispersion near the Fermi level. We also calculated a hypothetical dodecaboride  $\text{BB}_{12}$  (isoelectronic with  $\text{YB}_{12}$ ), where an yttrium atom is replaced by an "additional" boron atom, see Fig. 1. It was found that (i) some s,p- states of the "additional" boron atom are located in the vicinity of  $E_F$ ; (ii) the system is of a metal-like character with a rather high density of states at the Fermi level ( $N(E_F) = 3.034$  eV/cell), the main contribution being from the B2p states ( $\sim 72$  percentage).

As noted above, the experiments were reported recently, in which boron transforms from the usual non-metal to the SC state at high pressures (above 160 GPa), the crystal structure of the SC boron remains unknown [6]. This finding was explained [6] on the basis of the electron-phonon mechanism in the assumption that under high pressure -boron undergoes structural transformations to a simple fcc B having a metal-like energy spectrum, with  $N(E_F) = 0.154$  states/eV cell (lattice constant 2.44 Å) and the dominant contributions from the B2p states ( $\sim 60$ percentage). According to Table 2, the near-the Fermi level regions of our hypothetical systems  $\text{EB}_{12}$  and  $\text{BB}_{12}$  have a similar band structure. The former system can be interpreted as a model of elemental boron with a disordered lattice. The latter imitates the role of inter-icosahedral boron atoms in crystal. This allows us to surmise that the observed [9] transition of the rhombohedral  $\beta$ -boron to the superconducting state may be due both to lattice disordering and partial frustration of the initial icosahedral units, when some boron atoms take inter-icosahedral positions as a result

of high pressure. Such processes can be more probable than the phase transformation of rhombohedral -boron to the fcc structure proposed in [8] if we take into consideration the high cohesion properties of elemental boron [5-7].

### 3.2. $\text{YB}_6$

Fig. 1 presents the electronic band structure of Y hexaboride. The 10 occupied energy bands is made up by hybrid B2s,p-states represented the inter- and intra-octahedral B-B bonds. The VB width in  $\text{YB}_6$  (without quasi-core B2s band) is about 11.80 eV. The highest fully occupied bands is due to  $\text{Bp}_{x,y}$ -states formed by inter-octahedral interactions. They have strong dispersion along  $\Gamma$ -X direction due to the formation of hybrid Y-B bonds. The DOS spectrum has two maxima (A and B, Fig. 2), corresponding to hybrid states, formed by covalent B B bonds inside and between  $\text{B}_6$  clusters. This feature is typical for all  $\text{CaB}_6$  like hexaborides [15-17]

. The partially occupied band contains a considerable contribution from cation states and has also a large wave-vector dependence, which reflects the delocalized character of Yd states forming the bottom of the conductivity band.

It has been indicated that  $\text{YB}_{12}$  and  $\text{YB}_6$  are the conventional low-temperature phonon-mediated BCS superconductors, review [3]. Thus, the important parameter is the orbital composition of  $N(E_F)$ . According to our data, the lowering of the transition temperature (7.1 K ( $\text{YB}_6$ )  $\rightarrow$  4.7 K ( $\text{YB}_{12}$ )) can be explained by a considerable decrease of contributions of Yd-states to  $N(E_F)$  from 0.798 ( $\text{YB}_6 \sim 71$  percentage) to 0.538 ( $\text{YB}_{12}$ ,  $\sim 35$  percentage per atom in unit cell, Table 2).

### 3.3. $\text{YB}_2$ as compared with $\text{MgB}_2$

The electronic structures of layered  $\text{AlB}_2$ -like Mg and Y diborides are of a completely different, Fig. 3, 4. The peculiarities of the band structure of the SC  $\text{MgB}_2$  are due to the B2p states which form four  $\sigma(2p_{x,y})$  and two  $\pi(p_z)$  bands, Fig. 3. The  $E(\mathbf{k})$  dependence for B2p $_{x,y}$  and  $2p_z$  bands differs considerably. For B2p $_{x,y}$  like bands the most pronounced dispersion of  $E(\mathbf{k})$  is observed along the direction  $k_{x,y}$  ( $\Gamma$  - K of the Brillouin

zone (BZ)). These bands are of the quasi two dimensional (2D) type. They form a flat zone along  $k_z$  ( $\Gamma$ -A) and reflect the distribution of  $\sigma(2p_{x,y})$  states in the boron layers. These states make a considerable contribution to the  $N(E_F)$  forming metallic properties of the diboride.  $E_F$  is located in the region of bonding states and, the conductivity of  $MgB_2$  is due to hole carriers. Mg is ionized, the charge transfer takes place in the direction  $Mg \rightarrow B$ .  $B2p_z$ -like bands are responsible for weaker  $\pi(p_z)$  interactions. These 3D-type bands have the maximum dispersion in the direction  $k_z$  ( $\Gamma$ -A). Mgs,p and Bs states are admixed to  $B2p$ -like bands near the bottom of the VB and in the conduction band. Therefore the peculiarities of the electronic properties of  $MgB_2$  are associated with the metal-like 2p states of boron atoms located in plane nets. These states determine the DOS in the vicinity of the Fermi level and is an important condition for superconductivity in  $MgB_2$  and related phases [2,3, 19-21].

Thus the crucial features of the band spectrum of  $MgB_2$  for its superconducting properties (see also [2,3,19-21]) are: (i) the position of  $\sigma(p_{x,y})$  bands relative to  $E_F$  (the presence of hole  $p_{x,y}$ -states); (ii) their dispersion in the direction  $\Gamma$  - A ( $\Delta E^\sigma(\Gamma$ -A) is determined by the interaction between metal-boron layers); (iii) the value and orbital composition of  $N(E_F)$  (the main contributions from boron  $\sigma$  -states).

Let us compare the band structures of  $MgB_2$  and  $YB_2$ . The most obvious consequence of the metal variation ( $MgB_2 \rightarrow YB_2$ ) is band filling change caused by the increased number of valence electrons. For  $YB_2$ , the Fermi level is shifted towards a pseudogap between bonding and antibonding states. As a result, the near- $E_F$  spectra of  $YB_2$  and  $MgB_2$  differ radically. For  $YB_2$ , (i)  $\sigma(p_{x,y})$  boron bands are almost filled and the hole concentration is very small (near point A of the BZ, Fig. 3); (ii) the covalent d-p metal-boron bonding increases considerably and the  $B2p$ -like bands are shifted downwards to point K (these interactions are also responsible for the appearance of pronounced dispersion of bands in the direction  $\Gamma \rightarrow$  - A and for 2D  $\rightarrow$  3D transformation of the near- $E_F$  states); (iii) the Y4d band along the  $\Gamma$  -M is below  $E_F$  and these states give a large ( $\sim$

59 percentage) contribution to  $N(E_F)$ .

The 2D  $\rightarrow$  3D transformation of the near-  $E_F$  states can be also traced by comparing the the Fermi surfaces (FS) of  $MgB_2$  and  $YB_2$ , Fig. 3. For  $MgB_2$ ,  $B2p_{x,y}$  bands form two hole-like cylindrical Fermi surfaces around the  $\Gamma$  - A direction. The other tubular surfaces come from bonding (hole-like) and antibonding (electron-like)  $B2p_z$  bands. By contrast, the FS of  $YB_2$  consists of hole-like ellipsoids around the  $\Gamma$  - A line and 3D figures with electron-type conductivity. All these FSs are defined by mixed Y4d- $B2p$  states. Thus, the absence of superconductivity in  $YB_2$  can be accounted for (see also [21]) by the high energy shift of  $E_F$ , a considerable increase of Y4d-component in  $N(E_F)$ , and the absence of  $\sigma(p_{x,y})$  hole states at  $\Gamma$ , Fig. 3.

#### 4. Conclusions

We presented the results of full-potential LMTO band structure calculations for yttrium dodeca- and hexaborides compared with layered non-superconducting  $YB_2$  and the new "medium- $T_c$ " SC  $MgB_2$  diborides.

The band structures of boron-rich crystals are determined by the complicated intraatomic bonds including intra and between boron polyhedra ( $B_{12}$  for  $YB_{12}$  and  $B_6$  for  $YB_6$ ) and direct Y-B bonds. The DOS at the Fermi level for the low-temperature SC  $YB_{12}$  and  $YB_6$  has a similar composition and includes the large contribution of Y4d-states. The lowering of  $T_c$  ( $YB_6 \rightarrow YB_{12}$ ) can be explained by a considerable decrease in main contributions of Yd-states to  $N(E_F)$ . We performed also band structure calculations for two hypothetical structures: "dodecaboride" with an empty Y-sublattice ( $EB_{12}$ ) and the icosahedral phase ( $BB_{12}$ ), which is a result of the  $Y \rightarrow B$  substitution. Both crystals are metals with high DOS at the Fermi level. We speculate that the observed [9] transition of the rhombohedral  $\beta$  -boron to the superconducting state can be due to both lattice disordering and partial frustration of the initial icosahedral units as a result of high pressure. Such processes can be more energetically favorable than the phase transformation of rhombohedral  $\beta$  -boron to the

fcc structure proposed in [8].

Quite different are the band structures of layered  $\text{AlB}_2$ -like Mg and Y diborides. They are determined by intra- and interlayer interactions of plane (Mg,Y) and boron nets. In contrast to  $\text{MgB}_2$ , for  $\text{YB}_2$  the increase of covalent d-p bonding leads to the downward shift of  $\text{B}2p_z$  bands, larger dispersion of  $\sigma$  bands in the direction  $\Gamma - A$  and  $2D \rightarrow 3D$  band transformation near-  $E_F$ . The most crucial changes are connected with the increase of electron numbers resulting in the almost filled  $\sigma(p_{x,y})$  boron bands. The hole  $\sigma(p_{x,y})$  bands are absent at point and the density of states at the Fermi level is mainly defined by Y4d states, so these band structure peculiarities may be considered to be responsible for the absence of medium- $T_c$  superconductivity in  $\text{YB}_2$ .

## REFERENCES

1. J. Nagamatsu, N. Nakagawa, T. Muranaka, Y. Zenitani, J. Akimitsu, Nature 410 (2001) 63.
2. A.L. Ivanovskii, Russ. Chem. Rev. 70 (2001) 717.
3. C. Buzea, T. Yamashita, Superconductors, Science and Technol. 14 (2001) R115.
4. The Chemistry of Boron and Its Compounds (Ed. E.L. Muetterties), Wiley, New York, 1967.
5. S. Lee, D.M. Bylander, L. Kleinman, Phys. Rev. B42 (1990) 1316.
6. C. Maihiot, J.B. Grant, A.K. McMahan, Phys. Rev. B42 (1990) 9033.
7. D. Li, Y-N. Xu, W.Y. Ching, Phys. Rev. B45 (1992) 5895.
8. D.A.Papaconstantopoulos, M.J. Mehl, cond-matter/0111385 (2001).
9. M.L. Eremets, V.V. Struzhkin, H.K. Mao, R.J. Hemley, Science 203 (2001) 272.
10. Yu.B. Kuzma, Crystal chemistry of borons (in Russia), Vyssha Shkola, Lviv, 1983.
11. S.Y.Savrasov, Phys. Rev. B54 (1996) 16470.
12. M.Methfessel, M. Scheffler, Physica B. 172 (1991) 175.
13. J. P. Perdew and Y. Wang, Phys. Rev. B45 (1992) 13244
14. J.P. Perdew, S. Burke and M. Ernzerhof, Phys. Rev. Lett. 77 (1996) 3865.
15. H. Hasegawa, A. Yanase, J. Phys. C: Solid State Phys. 12 (1979) 5431.
16. H. Ripplinger, K. Schwarz, P. Blaha, J. Solid State Chem. 133 (1997) 51.
17. S. Massidda, A. Continenza, T. M. DePascale, R. Monnier, Z. Phys. B - Condensed Matter. 102 (1997) 83.
18. A.L. Ivanovskii, S.V. Okatov. Mendeleev Commun. 11 (2001) 8.
19. J.M. An, W.E. Pickett, Phys. Rev. Letters, 86 (2001) 4366.
20. J. Kortus, I.I. Mazin, K.D. Belashenko, V.P. Antropov, L.L. Boyer. Phys. Rev. Letters. 86 (2001) 4656.
21. N.I. Medvedeva, A.L. Ivanovskii, J.E. Medvedeva, A.J. Freeman. Phys. Rev., B64 (2001) 020502(R).

Table 1

Transition temperatures ( $T_c$ , K), structure type and lattice constants ( $\text{\AA}$ )  $\text{YB}_{12}$ ,  $\text{YB}_6$ ,  $\text{YB}_2$  and  $\text{MgB}_2$ .  $a$  and  $c$  are lattice parameters from [10],  $a^*$  and  $c^*$  are lattice parameters from our self-consistent data.

Boron	$T_c$	Structure type (space group)	$a$	$c$	$a^*$	$c^*$
$\text{YB}_{12}$	4.7	$\text{UB}_{12}(\text{Fm}3\text{m})$	7.5000	-	7.5223	-
$\text{YB}_6$	7.1	$\text{CaB}_6(\text{Pm}3\text{m})$	4.1132	-	4.1554	-
$\text{YB}_2$	—	$\text{AlB}_2(\text{P6}/\text{mmm})$	3.3036	3.8427	3.2116	4.0080
$\text{MgB}_2$	$\sim 40$	$\text{AlB}_2(\text{P6}/\text{mmm})$	3.083	3.521	3.0487	3.4664

Table 2

Total and site-projected  $l$  - decomposed DOS at the Fermi level (state/eV/cell) for borides.

Boride	Total	Ms	Mp	Md	Bs	Bp
$\text{YB}_{12}$	1.458	0.005	0.003	0.532	0.033	0.885
$\text{EB}_{12}$	6.177	0.240			0.033	5.904
$\text{BB}_{12}$	3.034	0.743	0.119		0.109	2.063
$\text{YB}_6$	1.130	0.017	0.020	0.798	0.001	0.294
$\text{YB}_2$	1.665	0.042	0.106	0.983	0.006	0.528
$\text{MgB}_2$	0.719	0.040	0.083	0.138	0.007	0.448

#### Figures.

- Fig.1. Band structures of  $\text{YB}_{12}$  (I),  $\text{EB}_{12}$  (II),  $\text{BB}_{12}$  (III) and  $\text{YB}_6$  (IV).  
 Fig.2. Total and partial DOS (1- s, 2 - p, 3 - d) for  $\text{YB}_{12}$ ,  $\text{EB}_{12}$  and  $\text{YB}_6$ .  
 Fig.3. Band structure and Fermi surface for  $\text{YB}_2$  (I) and  $\text{MgB}_2$  (II).  
 Fig.4. Total and partial DOS (1-s, 2 - p, 3 - d) for  $\text{YB}_2$  (I) and  $\text{MgB}_2$  (II).

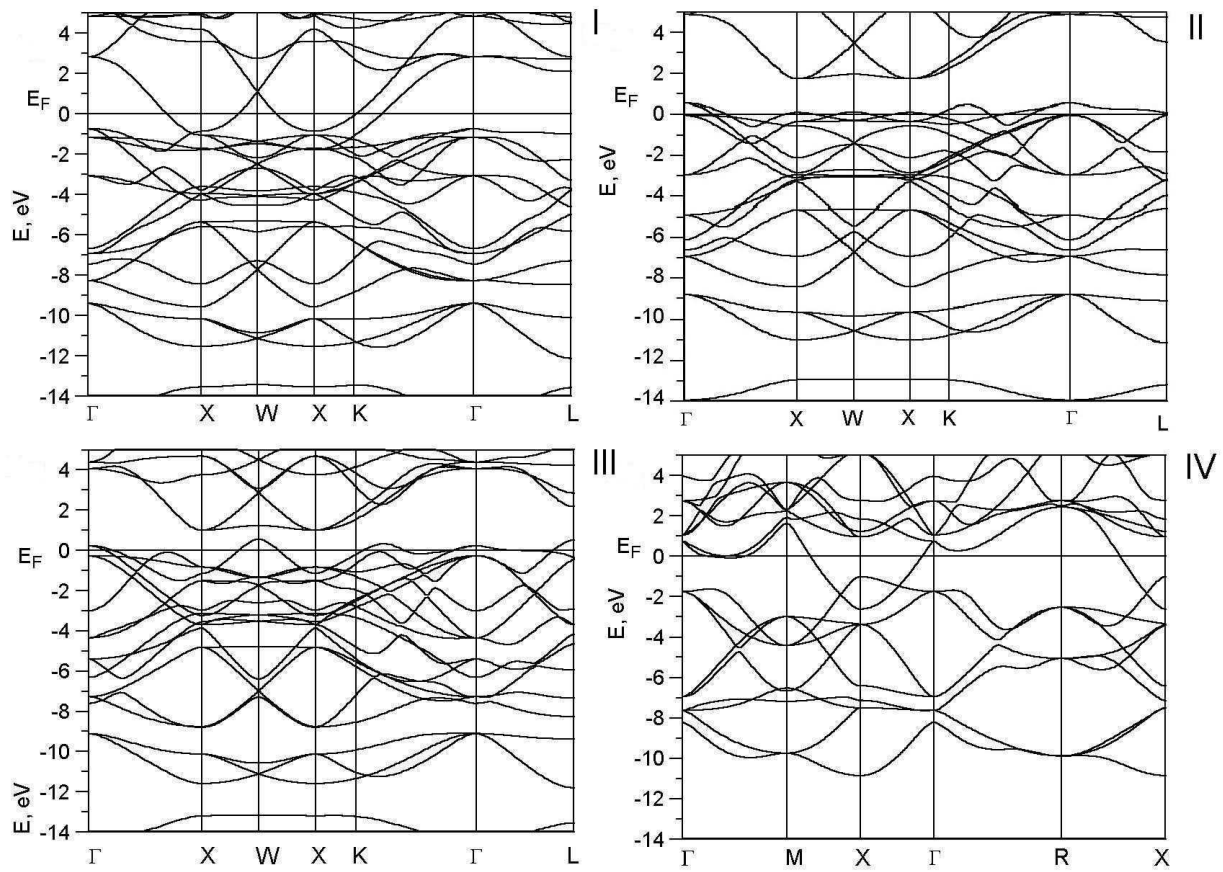


Fig.1.

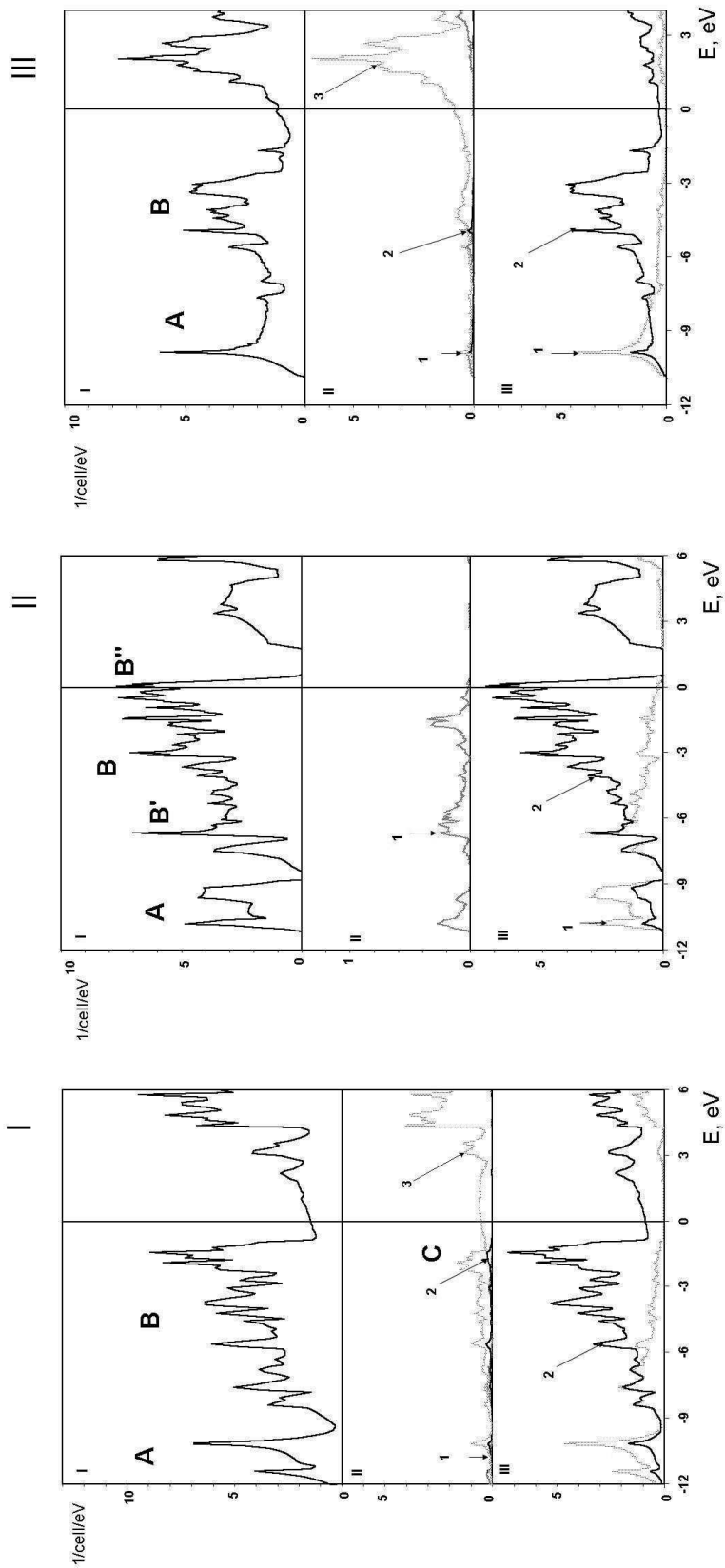
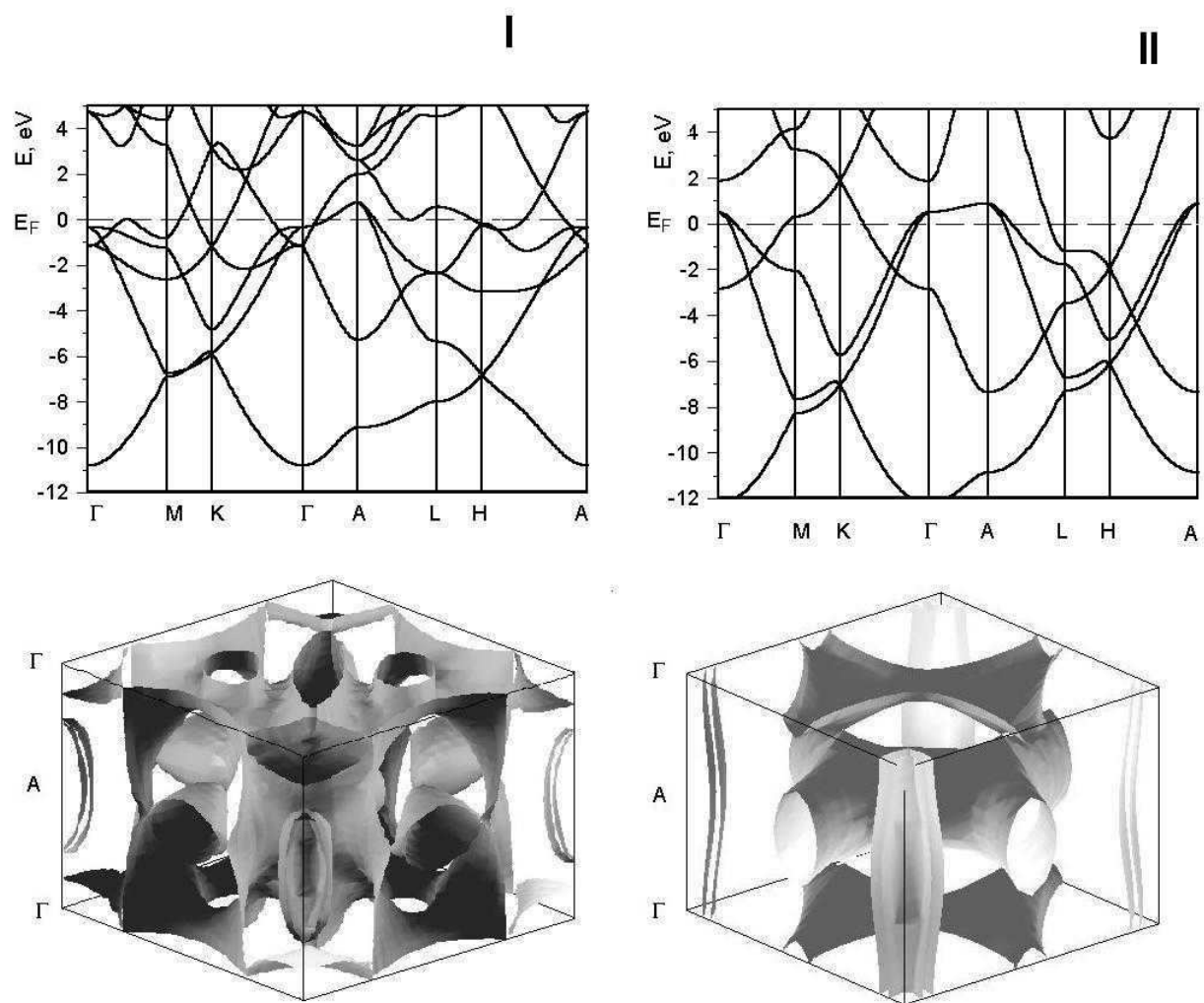


Fig.2.



**Fig.3.**

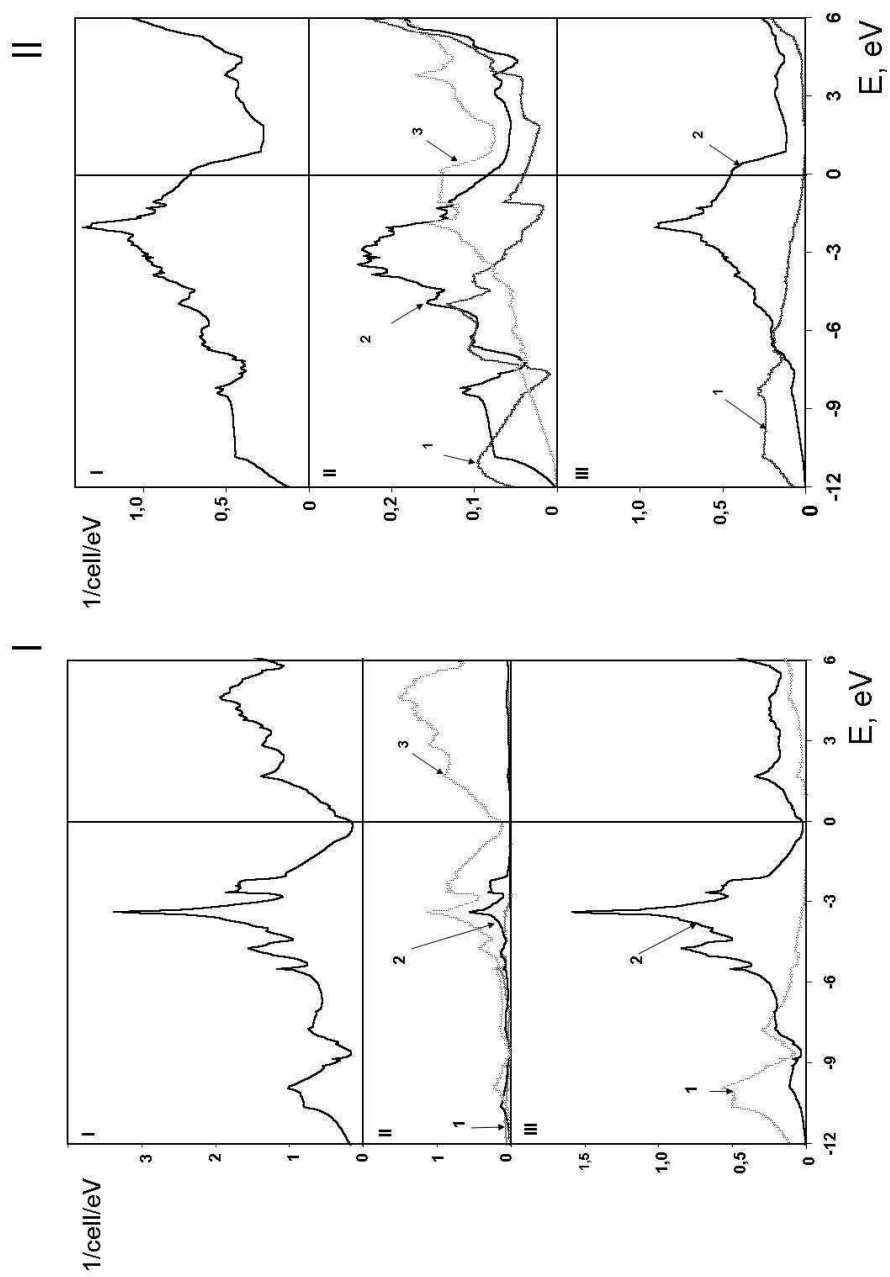


Fig.4.